Line Matching across Catadioptric Images under Short-Baseline Motion

Saleh Mosaddegh, David Fofi, Pascal Vasseur, Samia Ainouz

Line Matching across Catadioptric Images under Short-Baseline Motion

Saleh Mosaddegh[1], David Fofi[1], Pascal Vasseur[2], Samia Ainouz[1]

[1]Le2i UMR CNRS 5158, IUT Le Creusot, Université de Bourgogne, France
[2]MIS, Université de Picardie Jules Verne, Amiens, France

Abstract. Line matching across catadioptric images using line intersections with focus on short baseline motion of the imaging system is proposed. The relationship between images of constructing lines of an intersection on unitary sphere is studied and angle consistency and antipodal consistency are introduced as two useful properties which can be employed to find putative intersections correspondence and remove the outliers. The necessary equations for adapting boundary of a rectangular patch to the geometry of the catadioptric images are also derived and a standard correlation is used for measuring similarities of the intersections. Experimental results on both synthetic and real images are also presented.

1 Introduction

Line matching is simply finding the corresponding images of the same 3D line across two or multiple images of a scene. It is often the first step in the reconstruction of scenes such as an urban scene. The images can be captured by a perspective camera or a catadioptric system. The latest work which significantly improves on the state of the art for line matching across two or more perspective views was done in [1]: for each segment in one image, using correlation function a matching score is computed for all segments of the second image which are located inside the two epipolar lines of the two endpoints of the segment in the other image. Finally, the pair of segments with the best score is kept as the correct match. The most related work to line matching in catadioptric imaging systems is done in [5] for visual servoing/tracking purposes by tracking line features during the camera (and/or the object) motion. The interaction matrix (or image Jacobian) plays a central role to design vision-based control law. It links the variations of image observations to the camera velocity. The paper is mainly concerned with the use of projected lines extracted from central catadioptric images as input of a visual servoing control loop. However the method is based on the estimation of the partial camera displacement between two views, given by the current and desired images and it is entirely different from the problem of matching lines across views in which there is considerable movement and rotation between corresponding lines which is the subject of our work.

Our method for line matching consists of three main steps. First, lines of interest have to be detected in the images. Second, the line intersections (as salient interest points) are mutually compared and the lines belonging to the most similar ones are paired into the corresponding lines. Not always all the matches are correct and some lines are often matched incorrectly. These mismatches, called outliers, have to be removed which is the final stage of the line matching algorithm. As a further step, one may also be interested in computing the translation and rotation parameters of catadioptric system from the set of corresponding lines.

In this work, we are interested in the last two steps of the matching algorithm (for the first step, we use the algorithm which is explained in [9]). We use a window to measure similarities between intersection points. It is a well known fact that rectangular windows, usually used for cameras with perspective projections, are no longer appropriate for catadioptric cameras with a nonlinear projection [5,7]. We will tackle this problem by finding appropriate window boundaries using projection of a rectangular window in 3D space to catadioptric image using unitary sphere model. We will derive the related equations for the case of a paracatadioptric system, without loss of generality. Similarities between intersection points are determined by computing the 2D correlation. For outliers removal, we suggest checking angle consistency and antipodal consistency of intersections points which will shortly be explained.

The rest of this text is organized as follows. First, we derive the relation between normal vector of the great circle of any 3D line represented in the first unitary sphere coordinate system and its corresponding vector expressed in the second system. In section 3 we introduce appropriate matching windows suitable for comparing patches around an intersection. Section 4 details an algorithm for line matching across catadioptric images with a pure unknown rotation matrix and final section presents some experimental results of applying the proposed algorithm on both synthetic and real images. We skip giving the definition of catadioptric imaging systems and unitary sphere model due to space restrictions. We suggest references [2,3,4] for explanations and details.

Unless we explicitly mention, by “line” we refer to the normal vector of the plane which pass through the centre of unitary sphere and a 3D line in the scene. Also an “intersection” is a unit vector pointing from the centre of the unitary sphere toward the intersection of projections of two 3D lines on the unitary sphere. An “intersection point” is the intersection point of images of two 3D lines on the image plane. And finally, the angle between the great circles of two lines is referred as the “intersection angle”.

2 Finding Relation between Lines

Suppose line $\mathbf{n}_1$ is the corresponding line of line $\mathbf{n}_2$ (Fig. 1). A logical question can be: knowing a set of correspondences such as $\mathbf{n}_1$ and $\mathbf{n}_2$, is it possible to extract the transformation matrix between two positions of the imaging system? To answer this question we need to drive the relation between $\mathbf{n}_1$ and $\mathbf{n}_2$. We will show that:

Proposition 1. *The relation between two corresponding lines depends on not only the transformation* **R** *and* **t** *between two imaging systems but also on the direction of the 3D line.*

Proof. Consider a line in 3D scene with two separate 3D points $\mathbf{X}_1$ and $\mathbf{X}_2$ on it. Suppose $\mathbf{n}_1$ is the normal vector of the plane which pass through these two points and the origin of the first unitary sphere and $\mathbf{n}_2$ is the corresponding vector expressed with respect to the second camera (Fig. 1). Then:

$$\begin{aligned}\mathbf{n}_2 = (\mathbf{R}\mathbf{X}_1 + \mathbf{t}) \times (\mathbf{R}\mathbf{X}_2 + \mathbf{t}) = \dots \\ \det(\mathbf{R})\,\mathbf{R}^{-t}(\mathbf{X}_1 \times \mathbf{X}_2) + [\mathbf{t}]_\times \mathbf{R}(\mathbf{X}_1 - \mathbf{X}_2) = \dots \\ \det(\mathbf{R})\,\mathbf{R}^{-t}\mathbf{n}_1 + [\mathbf{t}]_\times \mathbf{R}(\mathbf{X}_1 - \mathbf{X}_2) = \mathbf{R}^*\mathbf{n}_1 + [\mathbf{t}]_\times \mathbf{R}(\mathbf{X}_1 - \mathbf{X}_2)\end{aligned} \quad (1)$$

Where metric transformation of the catadioptric system (represented by two unitary spheres in Fig. 1) is defined by the rotation matrix **R** and translation vector **t** and $\mathbf{R}^*$ denotes the co-factor matrix of **R**. □

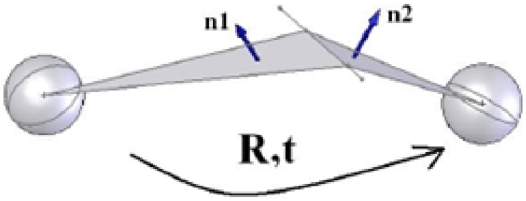

Fig. 1. 3D Line in the scene and its projections on a unitary sphere at two different positions. $\mathbf{n}_1$ and $\mathbf{n}_2$ are normal vectors of great circles.

Therefore if transformation between two positions of the imaging system is a pure rotation ($\mathbf{t}$=$\mathbf{0}$) or the movement of the system in comparison to its distance to the scene is very small (short baseline, for example aerial imaging), we can neglect the second term in (1) and conclude that:

Corollary 1. *In the case of pure rotation or short base line,* $\mathbf{n}_1$ *and* $\mathbf{n}_2$ *are related by the co-factor matrix of the rotation matrix.*

$$\mathbf{n}_2 = \mathbf{R}^*\mathbf{n}_1 \quad (2)$$

One immediate result of above statement is that for the case of short baseline, having minimal three line correspondences, we can find $\mathbf{R}^*$ and then find the rest of line correspondences.

3 Adaptation of a Rectangular Window to the Catadioptric Image Geometry

Rectangular windows commonly used for matching in perspective projections are not suitable for the catadioptric systems [6,7]. Therefore derivation of an appropriate window is necessary. In this section, we will drive the relation between any pixel of a perspective image taken from the 3D scene with the viewpoint coincident on the focal point of a paracatadioptric mirror and its corresponding pixel on the paracatadioptric image plane by help of unitary sphere model. The generalization to the other types of mirror is similar.

We are particularly interested in studying a patch with its centre on the intersection of two lines in the catadioptric image. Later in section 4 we use the result of this section to extract and compare patches around intersections in two images in order to find corresponding intersections.

Consider a small perspective image taken from surroundings of an intersection in 3D scene by positioning the focal point of a perspective camera at the origin of the unitary sphere and pointing the camera at the direction of the intersection (the axis of the camera coincident with the line connecting the origin of unitary sphere and the intersection point). Projection of this window on the unitary sphere creates a small patch that, projected to the image plane, gives us the desired window for matching (See Fig. 2).

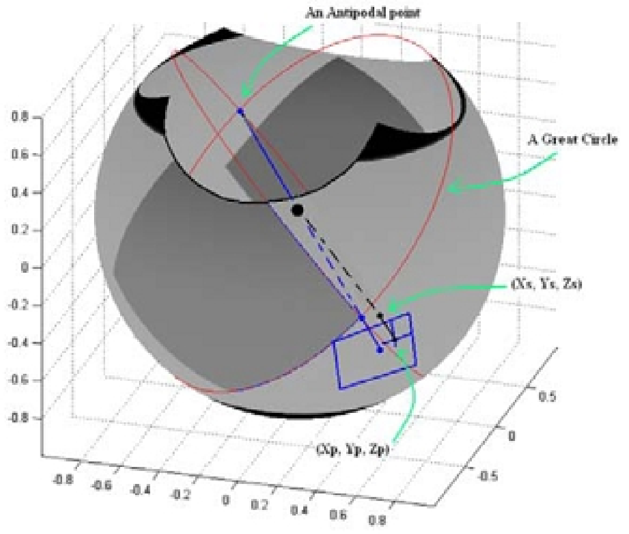

Fig. 2. Projection of a pixel of the perspective window onto the unitary sphere. Examples of an antipodal point and two great circles are also depicted here.

From system intrinsic parameters, all that is needed is the image coordinates of the centre of the paraboloid and its radius h. Both these quantities are measured in pixels from a single omnidirectional image. The viewing direction is the same as the direction of the intersection and a reasonable patch size (resolution, the number of desired pixels in each dimension of the window) and effective focal length (zoom factor, the distance of the window from the viewpoint of the mirror) of the desired perspective window should be set. Again, all these quantities are specified in pixels. For each three-dimensional pixel location $\mathbf{P} = \left[X_p \; Y_p \; Z_p \right]$ on the desired perspective window, its intersection with unitary sphere is the normalized vector $\mathbf{P} = {}^{\mathbf{P}}/_{\|\mathbf{P}\|} = {}^{\mathbf{P}}/\sqrt{X_p^2+Y_p^2+Z_p^2}$. Using intrinsic parameters of paracatadioptric system and after some manipulation of unitary sphere equations, it can be shown that the pixel position $(i,\, j)$, the projection of point $\mathbf{P}$ on sphere into image plane is:

$$i = \frac{f\alpha}{1 - Z_s} X_s + C_x \; and \; j = \frac{f}{\alpha\,(1 - Z_s)} Y_s + C_y \tag{3}$$

Where (C_x, C_y) is the principal point of the image plane, α is the parameter describing the mirror shape and f is the focal length. The above computation is repeated for all points in the desired perspective window (Fig. 2).

4 An Algorithm for Line Matching across Catadioptric Images with a Pure Unknown Rotation Matrix

In this section, we focus on matching line intersections for the case of pure rotation and short baseline motion and show how it can lead us to compute the rotation matrix and at the same time finding line correspondences. Our approach consists of the following steps:

We will explain these steps in details in the rest of this section.

4.1 Extracting Lines and Finding Intersections

We use the algorithm proposed in [9] for extraction of lines from catadioptric images. Images of lines are conics and two general conics intersect each other at two points which are called antipodal points when projected onto the unitary sphere. From extracted lines we find all possible intersection points inside the image plane. We focus on line intersections as salient points for some of their interesting properties which can help us to match them more efficiently as well as to remove mismatches from the set of putative matches. We call these properties *angle consistency* and *antipodal consistency*. Angle consistency is defined and proved as follows.

Proposition 2. *The intersection angle of two corresponding intersections points are identical if the motion of the imaging system is a pure rotation.*

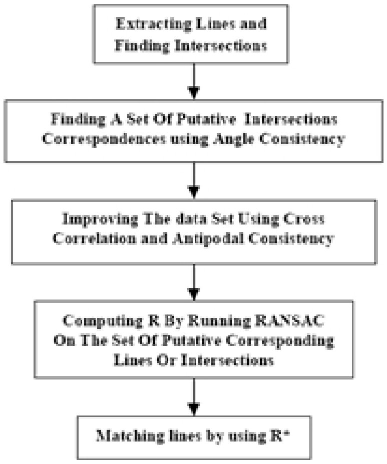
Extracting Lines and Finding Intersections
Finding A Set Of Putative Intersections Correspondences using Angle Consistency
Improving The data Set Using Cross Correlation and Antipodal Consistency
Computing R By Running RANSAC On The Set Of Putative Corresponding Lines Or Intersections
Matching lines by using R*

Fig. 3. The proposed algorithm for line matching across catadioptric images with a pure rotation.

Proof. The angle between images of two 3D lines on the unitary sphere is the angle between two planes which pass through centre of sphere and any of lines. Since in the case of pure rotation, the centre of sphere does not move, and also lines are fixed in the scene, the angle also do not change after the rotation of the imaging system. □

By antipodal consistency, we refer to the fact that if two intersections in two images are correspondences then their antipodal points should also match. Fig. 2 and Fig. 6 show examples of antipodal points on the unitary sphere and image plane respectively. Another motivation for working with intersection points is that the orientation of lines can be employed to remove cyclo-rotation[1] of the image around an intersection point. Consider the intersection point of the synthetic scene in Fig. 4 in which there is a pure rotation around the mirror focal point between two images.

The constructing lines of the intersection divide its surrounding into four patches. Assuming a rigid scene and for the case that the motion of the imaging system consists of only a rotation around mirror centre or it is a short range motion, the parts of the scene behind the all four patches remain the same with the motion of the system (in fact this is true for every point of scene among them intersection points). Therefore to extract a patch around each intersection point to feed into similarity measuring function such as correlation in order to compare two intersections, it is sufficient to consider a window with the centre of window located on the intersection point and extract two patches by aligning the window to the orientation of two lines of the intersection in order to remove

[1] Rotation about the symmetry axis of the mirror.

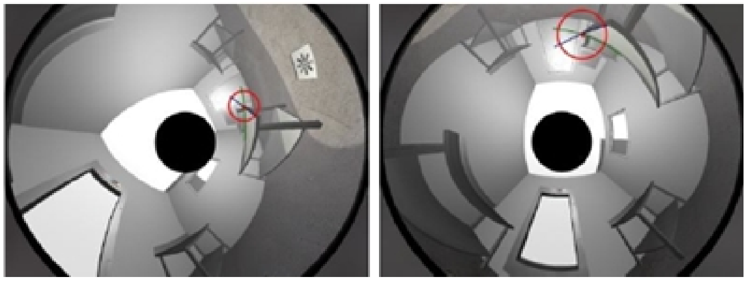

Fig. 4. A synthetic rigid scene. There is a pure rotation around the mirror focal point between two images. The scenes behind the all four patches remain the same.

cyclo-rotation (Fig. 5). The necessary equations for adaptation of the patch to the geometry of the catadioptric image was already derived in section 3.

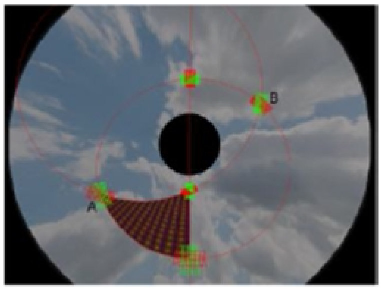

Fig. 5. Extraction of patches. Size and resolution are the same for all patches. Notice the alignment of patches with the lines and their adaptation to the geometry of the catadioptric image. An antipodal pair is also shown: Intersection B is the antipodal point of intersection A and vice versa.

4.2 Finding a Set of Putative Intersections Correspondences using Angle Consistency

Using angle consistency property, we are able to compute a putative set of correspondences by matching angles between two sets of intersections. Due to error in line extraction step, we need to consider an appropriate angle tolerance. In practice, along with mismatching, multimatching is very probable in this step and we need to remove mismatches as it will shortly be explained in next steps.

4.3 Improving a Set of Putative Intersections Correspondences

After finding a putative set of intersections, we continue with further removal of mismatches by using cross-correlation followed by checking mutual consistency and antipodal consistency of putative correspondences. In this step we assume that higher correlated patches make better pair than less correlated patches (this is not always true though and this assumption may fail if the scene includes highly repetitive patterns).

Measuring the Similarity between Putative Intersections Correspondences. By adapting patches to the geometry of the catadioptric image and by aligning them with lines, we can remove a considerable amount of distortion and we are able to improve our initial set of putative matches by measuring the similarity between patches. For this work we simply used normalized 2D cross-correlation function (simply CC). A patch moves pixel by pixel over the search window and a correlation coefficient is calculated in each position. The position where the correlation coefficient reaches its highest value is selected as a position of the best fit.

One should notice that we are not looking for the exact position of the best fit since all we need is to find the most similar patches. However we still should search for the highest correlation coefficient by moving the window around the intersection point because there is often considerable error in the position of the intersection point due to error in line extraction stage.

Fig. 5 shows a simple synthetic scene with three lines. In order to measure the similarity between two intersections, one of the patches of the first intersection is compared with both patches of the second intersection point and the highest score is retained as the similarity score of the two intersection points.

Pairing by Checking Mutual Consistency. A common method of pairing patches and eliminating mismatches is setting a minimum value (a threshold) for the correlation coefficient (setting a threshold does not mean that all the mismatches are eliminated). However in our work, a winner takes all scheme is employed which means the pair of patches with the best score is kept as the correct match. In this step, mutual correlation coefficients of all patches in two images are computed and arranged in a matrix with the number of rows and columns equal to the number of patches in the first and the second image respectively. Matches are accepted into the initial set of putative correspondences if they show a maximal correlation coefficient in both directions. In other words, if maximum of row r has been found at column c and the maximum of this column also lies in the row r then the patch r in the first image and the patch c in the second image are considered as a putative corresponding pair. This has the effect of removing patches which have multiple matches in other image. Moreover often a part of the scene may be visible in only one of the images. This will result in random or fake matches, since a correct match does not exist. This step also removes the random matches.

Further Outlier Removal by checking Antipodal Consistency. The aim of this step is to further remove mismatches based on the fact that if two intersection points are corresponding, their antipodal points should also be corresponding.

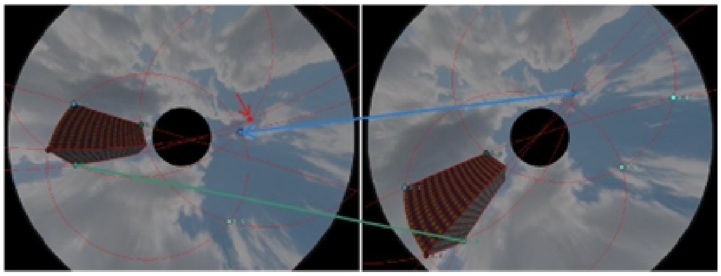

Fig. 6. An example of antipodal inconsistency. While the match shown by green color is a correct match, notice that the antipodal point of the intersection point in the right image has matched to a wrong intersection point on the left image (instead of antipodal point of its correspondence in the left image shown by a red arrow).

Therefore if two intersection points are matched but their antipodal points do not match with each other, we remove the correspondence from the list of putative matches. Fig. 6 shows an example of an antipodal inconsistency. Fig. 7 shows two synthetic catadioptric images and the final set of putative intersections correspondences.

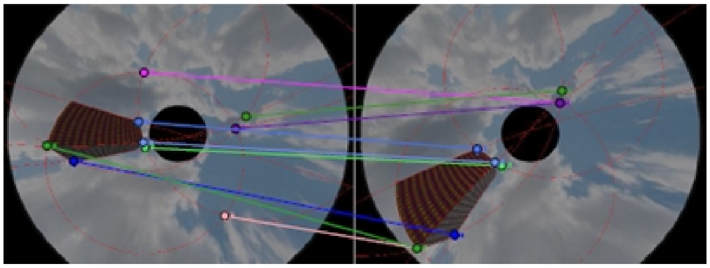

Fig. 7. An example of a set of putative intersections correspondences. There is only one mismatch).

4.4 Computing R by Running RANSAC on the Set of Putative Corresponding Lines or Intersections

We use RANSAC to find final correspondences, to remove the rest of outliers and to compute **R**. RANSAC is useful in the case that a lot of correspondences are provided, since its complexity does not depend on the total number of correspondences. In section 2 we derived the equation for the relation between the normal vectors of great circles of two corresponding lines. This equation serves as Fitting Function for our RANSAC algorithm. Knowing a putative intersection correspondence, it is easy to extract related putative lines correspondences by considering each line of the first intersection as a corresponding line for any of two lines of the second intersection and vice versa. We can also run RANSAC on the set of putative correspondences (intersections or lines). In this case we need to derive the equation for the relation between two corresponding intersections as follows:

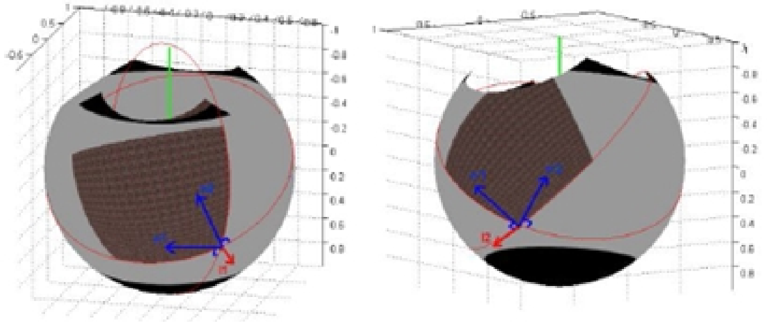

Fig. 8. Any intersection unit vector can be computed by taking the cross product of the normal vectors of great circles of its two constructing lines.

An intersection **I** can be computed by taking the cross product of the normal vectors of great circles of its two constructing lines, denoted by $\mathbf{n}_i^{'}$ in the following equation (Fig. 8). Therefore, the relation between two corresponding intersection and can be found as follows:

$$\mathbf{I}_2 = \mathbf{n}_1^{'} \times \mathbf{n}_2^{'} = (\mathbf{R}^*\mathbf{n}_1) \times (\mathbf{R}^*\mathbf{n}_2) = \mathbf{R}^{**}\left(\mathbf{n}_1 \times \mathbf{n}_2\right) = \mathbf{R}\mathbf{I}_1 \qquad (4)$$

Corollary 2. *In the case of pure rotation or short baseline, two corresponding intersections on the unitary sphere are related by a rotation matrix.*

4.5 Final Step: Matching Lines by means of R*

Knowing $\mathbf{R}^*$, matching lines between two images is straightforward. For each line in the first image, all which is needed to find its corresponding line in the second image is to multiply $\mathbf{R}^*$ at normal vector of great circle of the line. The result vector is pointing at the same direction as the normal vector of great circle of corresponding line is pointing. We may also drive $\mathbf{R}$ from $\mathbf{R}^*$ (by computing the cofactor matrix of $\mathbf{R}^*$) and correct the result matrix so that it represents a rotation matrix (for example using SVD so that its smallest singular value becomes zero).

5 Experimental Results

5.1 Synthetic Images

Fig. 9 shows the result of applying our line matching algorithm on the synthetic images of Fig. 7. The computed **R** is:

$$\mathbf{R} = \begin{bmatrix} 0.7567 & 0.6071 & -0.2428 \\ -0.6114 & 0.7886 & 0.0664 \\ 0.2318 & 0.0982 & 0.9678 \end{bmatrix} \tag{5}$$

Notice that there are several possible solutions for converting the matrix **R** to the Euler angles. In order to check the accuracy of the result we multiply the inverse of **R** matrix with the real rotation matrix of the imaging system (ground truth: 40 degrees of rotation around the z-axis and 15 degrees of rotation around the y-axis). The result should be close to the identity matrix as follows:

$$\mathbf{R}^{z}_{-40} \cdot \mathbf{R}^{y}_{-15} \cdot \mathbf{R}^{-1} = \begin{bmatrix} 0.9964 & 0.0195 & 0.0828 \\ -0.0315 & 0.9889 & 0.1453 \\ -0.0790 & -0.1474 & 0.9859 \end{bmatrix} \cong \mathit{identity\,matrix} \tag{6}$$

$\mathbf{R}^{k}_{d}$ means d degrees of rotation aroung k-axis.

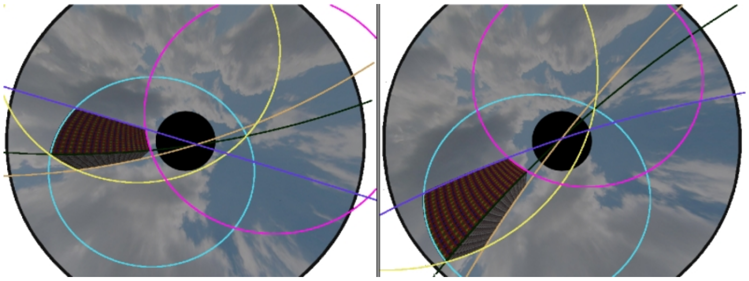

Fig. 9. The line correspondences computed by using matching frequency matrix. Each color represents a correspondence.

5.2 Real Images

The number of intersections is equal to the number of all possible selections of two lines from the set of lines in an image. This number increases very fast with the increase in the number of lines and can result in massive computational time during the correlation step. One solution can be to find real intersections by measuring the "corner response" of the intersections. One good "corner response" measuring function has been proposed in [10]. In this work we did not embed this part inside the proposed algorithm. However, to evaluate the performance of the method on real images, we reduced the number of lines by feeding the line detection algorithm with simple images consisting only prominent lines in the image.

Fig.10 shows the result of applying our algorithm on real images. Except one outlier, the rest of matches are correct. This result is the best result among four trials with different window sizes (20, 30, 40 and 50).

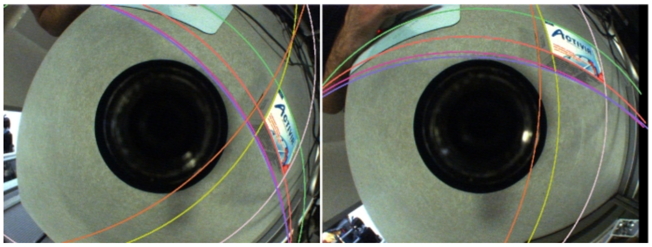

Fig. 10. Result of applying our method on a real image. Except one outlier (black colour), the rest of matches are correct.

The rotation matrix and one possible Euler angles combination for this pair of images are:

$$\mathbf{R} = \begin{bmatrix} 0.7620 & 0.6471 & -0.0008 \\ -0.6476 & 0.7620 & 0.0095 \\ 0.0068 & -0.0067 & 1.000 \end{bmatrix} \tag{7}$$

$$R_x = -2.3752^\circ,\ R_y = -0.2256^\circ,\ R_z = -41.9013^\circ$$

which are representing almost a pure rotation around z-axis and one can visually confirm the rotation by looking at both images. Unfortunately we do not have the real rotation of the imaging system but we tried to rotate the imaging system merely around its z-axis. Our implementation of the method suffers from using cross-correlation, a very weak similarity measuring tool for comparing patches. During our experiments we found that this function fails to detect correct patches when there is a considerable displacement and deformation between corresponding patches between two images. Fig. 11 shows the result of two experiments on both synthetic and real images. Notice the considerable amount of displacement and deformation between views. The number of correct correspondences in the case of synthetic images is higher thanks to the higher accuracy in extraction of lines.

6 Conclusions

This work was an opening effort on line matching in catadioptric images. In this work:

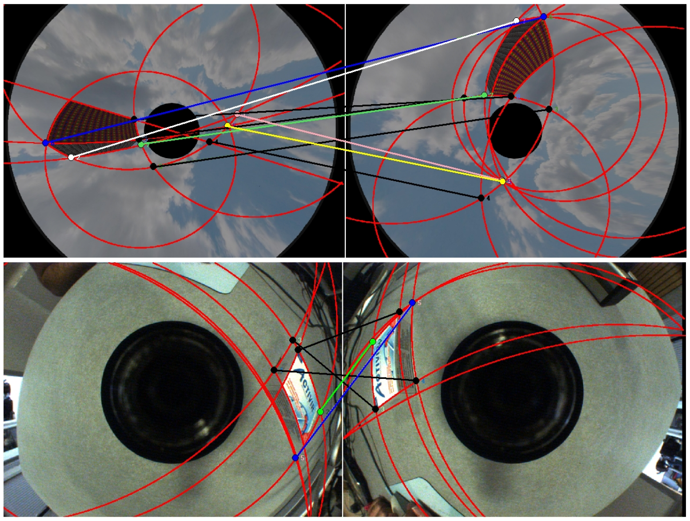

Fig. 11. The result of experiment on the images with considerable displacement and deformation between two views. The number of outliers (black colour) is high specially for real images due to deficiency of cross-correlation.

- The relation between normal vector of the great circle of any 3D line represented in the first unitary sphere coordinate system and its corresponding vector expressed in the second system was derived and it was shown that it is not possible to match lines by only knowing a set of such correspondences.
- Usage of line intersection points as salient points for matching lines in catadioptric images was proposed.
- The angle between constructing lines of an intersection was used as a measure for finding a putative set of intersection correspondences (Angle Consistency).
- It was shown that how the orientations of lines can be used to remove the cyclo-rotation of the image around an intersection points.
- The necessary equations for adapting boundary of a patch to the geometry of the catadioptric image were derived.
- Cross-correlation similarity measuring function along with adapted patches to the geometry of the catadioptric image was employed to remove wrong matches.
- The fact that if two intersection points are corresponding, their antipodal points should also match was employed for further removal of wrong matches (Antipodal Consistency).

Also an automatic line matching method was proposed for the case of pure rotation or short rang motion of the imaging system. During the experiments it was found that the high number of intersections could dramatically increase the computational time of the correlation step. Finding a solution for this problem can be the subject of future work.

One should notice that in this work we studied the problem of line matching in catadioptric images using intersections and we proposed a basic algorithm based on the result of this study. Further evaluation and optimization of the method is the subject of future work.

References

1. Schmid, C., Zisserman, A.: Automatic Line Matching across Views. In: Proc. of IEEE Conference on Computer Vision and Pattern Recognition, 666–672 (1997)
2. Barreto, J.P., Araujo, H.: Issues on the Geometry of Central Catadioptric Image Formation. In: Proc. of IEEE International Conference on Computer Vision, 422–427 (2001)
3. Baker, S., Nayar, S.: A Theory of Catadioptric Image Formation. In: Proc. of IEEE International Conference on Computer Vision, 35—42 (1998)
4. Geyer, C., Daniilidis, K.: Catadioptric Projective Geometry. International Journal of Computer Vision 45(3), 223–243 (2001)
5. Mezouar, Y., Haj Abdelkhader, H., Martinet, P., Chaumette, F.: Central Catadioptric Visual Servoing from 3D Straight Lines. In: IEEE/RSJ Int. Conf. on Intelligent Robots and Systems 1, 343–349 (2004)
6. Chahl, J., Srinivasan, M.: A Complete Panoramic Vision System, Incorporating Imaging, Ranging, and Three-dimensional Navigation. In: IEEE Workshop on Omnidirectional Vision, 104–111 (2000)
7. Svoboda, T., Pajdla, T.: Matching in Catadioptric Images with Appropriate Windows and Outliers Removal. In: Proc. of 9th Int. Conf. Computer Analysis of Images and Patterns, 733–740 (2001)
8. Mikolajczyk, K., Schmid, C.: A Performance Evaluation of Local Descriptors. In: International Conference on Computer Vision and Pattern Recognition (2003)
9. Bazin, J.C., Demonceaux, C., Vasseur, P.: Fast Central Catadioptric Line Extraction. In: Iberian Conference on Pattern Recognition and Image Analysis, 25–32 (2007)
10. Harris, C., Stephens, M.: A Combined Corner and Edge Detector. In: Proc. of 4th Aley Vision Conference, 147–151 (1988)